HHS Public Access

Author manuscript

Nat Neurosci. Author manuscript; available in PMC 2012 December 01.

Published in final edited form as:

Nat Neurosci. 2012 June ; 15(6): 905–912. doi:10.1038/nn.3106.

Gating and control of primary visual cortex by pulvinar

Gopathy Purushothaman[1], **Roan Marion**[1], **Keji Li**[2], and **Vivien A. Casagrande**[1,2]

[1]Department of Cell and Developmental Biology, Vanderbilt University

[2]Department of Psychology, Vanderbilt University

Abstract

The primary visual cortex (V1) receives its driving input from the eyes via the lateral geniculate nucleus (LGN) of the thalamus. The lateral pulvinar nucleus of the thalamus also projects to V1 but this input is little understood. We manipulated lateral pulvinar neural activity and assessed the effect on supra-granular layers of V1 that project to higher visual cortex. Reversibly inactivating lateral pulvinar prevented supra-granular V1 neurons from responding to visual stimulation. Reversible, focal excitation of lateral pulvinar receptive fields increased 4-fold the visual responses in coincident V1 receptive fields and shifted partially overlapping V1 receptive fields towards the center of excitation. V1 responses to regions surrounding the excited lateral pulvinar receptive fields were suppressed. LGN responses were unaffected by these lateral pulvinar manipulations. Excitation of lateral pulvinar after LGN lesion activated supra-granular layer V1 neurons. Thus, lateral pulvinar is able to powerfully control and gate information outflow from V1.

The primate visual system is currently viewed as a rough hierarchy of 30 or more cortical areas[1–4]. Area V1 is at the bottom of this hierarchy and contains a representation of important elementary visual features. Synaptic inputs from LGN as well as intracortical circuits are thought to underlie this key visual representation[1,2]. This model of visual system organization and function is incomplete in at least two aspects[4]. First, the model does not take into account the significant input to V1 from pulvinar in elucidating V1 function[4–7]. Second, unlike cortico-cortical connections, cortico-pulvino-cortical projections are not hierarchical[4]. Lateral pulvinar receives input from infra-granular layer 5 of V1 and projects to supra-granular layers 1–3 of V1 as well as to layers 3–4 of the secondary visual area V2[5,8–10]. Supra-granular layers 2–3 of V1 also project to granular layer 4 of V2 (Supplementary Fig. 1)[5]. Besides each sub-nucleus of pulvinar (e.g., lateral pulvinar) projecting both forward and backward to multiple interconnected cortical areas (e.g., V1 and V2), multiple sub-nuclei connect with the same cortical area[5]. In the absence of layers or columns within the sub-nuclei of pulvinar[5], this complex mesh of interconnections obscures the hierarchical position of pulvinar relative to V1 and V2[4]. Consequently, it is difficult to decipher the distinct function of each node along the cortico-pulvino-cortical pathway; it is

Author contributions

GP and VAC designed the experiments, all authors performed the experiments, GP analyzed the data and wrote the paper, all authors edited the manuscript, and VAC supervised the work.

also difficult to tease out the causal relationship between neural activity at different nodes[4,11].

Despite these complications, certain facts about the pulvinar nucleus make it necessary to address these two limitations. The pulvinar has expanded through evolution in proportion to the enlargement of higher visual and association cortices with which it connects[5–7]. Pulvinar lesions in monkeys and humans often result in profound visual deficits such as spatial neglect and impaired attention[12–20]. Human and monkey experiments have shown pulvinar activity to be correlated with aspects of spatial vision, visual salience, attention, and saccadic suppression[21–28]. Pulvinar atrophy is also characteristic of severe neuropsychiatric disorders and treatment of some of these disorders mitigates pathologies of the pulvinar[29]. That a single thalamic nucleus is associated with such a wide array of visual functions and causes such a variety of deficits when damaged are not easily explained. This motivates a better understanding of the position of pulvinar in the functional hierarchy of the visual system.

As a simple first step towards this goal, we studied the *net* effect of manipulating the activity of pulvinar neurons on their projection zone lowest in the cortical hierarchy, i.e., the supra-granular layers of V1. We locally excited or suppressed neural activity in the lateral sub-nucleus of pulvinar and measured the impact of these manipulations on the V1 target zone of the affected lateral pulvinar neurons. For comparison and control, we also monitored and manipulated LGN neural activity in similar manner.

Results

We measured the responses of neurons in superficial layers 2–3 of area V1 to high-contrast (50%) drifting sinusoidal gratings presented within the neurons' visual receptive fields (Methods and Supplementary Fig. 2). In each experiment, responses of multiple V1 neurons were simultaneously measured using a 100-electrode array implanted in one hemisphere. Receptive fields of neurons sampled by different electrodes of the array varied in size from 1° to 4° and were located within 6° of *area centralis* (AC). These measurements showed a characteristic brisk phasic response to onset of visual stimulation followed by a tonic response for the reminder of the stimulation (Fig. 1a).

Effect of reversible inactivation of lateral pulvinar

Using a microelectrode we found lateral pulvinar neurons whose receptive fields overlapped with a majority of V1 receptive fields sampled by the array. Centrally located lateral pulvinar receptive fields that satisfied this criterion varied in size from 1° to 6° and were within 6° of *area centralis*. We inactivated the lateral pulvinar neurons by infusing a small volume (0.5μL) of the GABA agonist Muscimol (Methods). We then repeated the V1 measurements. In 95% (156/164) of V1 neurons studied in 3 animals, the characteristic visually driven responses were almost completely abolished after the visuotopically matched region of lateral pulvinar was inactivated (Fig. 1a, b). This change occurred at all orientations of the sinusoidal grating (Fig. 1c). The average visual response decreased from 43.1 ± 2.9 spikes/sec (mean ± s.e.m) to 15.45 ± 1.8 spikes/sec (Fig. 1b), a significant change (Wilcoxon rank-sum test, P=0; n=164) of 64%. We quantified the visual responsiveness of

V1 neurons by computing the ratio of post-stimulus peak response to the pre-stimulus baseline (or background) response. This ratio changed significantly as a consequence of lateral pulvinar inactivation (Wilcoxon rank-sum test, P=0; n=164), with the average value decreasing by 300% from 4.01 ± 0.24 (mean ± s.e.m) to the near-baseline value of 1.34 ± 0.03 (Fig. 1d). Baseline V1 activity also changed significantly (Wilcoxon rank-sum test, P<0.001; n=164) decreasing by 36% after lateral pulvinar inactivation (inset, Fig. 1d).

After lateral pulvinar injection, the phasic component of V1 response was suppressed more strongly near the original preferred orientation of the neuron than near non-preferred orientations (Fig. 1e). We computed a suppression index as the divisive reduction in the ratio of the peak-to-baseline response that occurred with lateral pulvinar inactivation (Methods). Suppression at the preferred orientation (mean ± s.e.m = 0.11 ± 0.01) was about 5-fold stronger than at the half-width orientation (0.58 ± 0.10; Wilcoxon rank-sum test, P< 10^{-30}; n=164; Fig. 1f).

Spatiotemporal extent of the lateral pulvinar injections

To exclude cases in which the injection in lateral pulvinar diffused into the LGN or the thalamic reticular nucleus (TRN), we mixed the injected muscimol with biotinylated dextran amine (BDA) and probed it with Alexafluor-488 conjugated streptavidin (Methods). In the three cases described above, complete reconstruction of the thalamus showed the fluorescence was confined to lateral pulvinar within 500 μm of the injection, with no fluorescence in either the LGN or the TRN (Fig. 1g, Supplementary Figs. 3–4). Slight effusion along the path of injection observed in one case was also confined to dorsal lateral pulvinar and did not encroach on the TRN (Supplementary Fig. 4a).

Strong binding to $GABA_A$ receptors and high-affinity uptake into GABAergic neurons and astrocytes keep injected muscimol locally sequestrated[30,31]. Studies with [^{3}H] muscimol have found that even for large 1 μL injections of muscimol, the region of effectiveness remains confined to about 1 mm over several hours[30,31]. The 500 μm regions of fluorescence that resulted from 0.5 μL injections in our cases are in rough agreement with these measurements. However, some studies that used large volume (up to 2 μL) muscimol injections have reported that behavioural deficits sometimes changed or strengthened 1–2 hours after injection[32]. Effusion along the injection pipette or the slow spread of muscimol in the tissue at a rate of about 1–2 mm over 1–2 hours could account for these observations[32] (see Methods, “Injections”). To test the latter possibility, we studied the temporal dynamics of the effect of lateral pulvinar injections by measuring V1 visual responses in 15 minute intervals over several hours. These measurements showed that the average V1 visual response in the 15 minutes prior to the injection was 41.9 ± 6.1 spikes/sec (mean ± s.e.m). V1 visual responses started decreasing within a few minutes (< 5 min) of the injection and the average response between 20 min and 35 min after the lateral pulvinar injection was 10.4 ± 2.4 spikes/sec (Supplementary Figs. 5a), a significant change (Wilcoxon rank-sum test, P<10^{-9}; n=36) of 75% from the pre-injection response. Notably, there was no significant change in V1 visual responses thereafter for up to 125 minutes after the injection (Wilcoxon rank-sum test, P>0.4; Supplementary Fig. 5b, c,d; see also Supplementary Fig. 6). Because the LGN was 1.5–2.0 mm from the centre of the injection at

the closest approach in our cases (Fig. 1g, Supplementary Figs. 3 and 4), at the rate of diffusion implied by the above-mentioned behaviour studies (~1 mm/hour), changes in V1 responses due to leakage into LGN could not have occurred sooner than 60–90 minutes after the injection. Therefore, in addition to the histology, this analysis also showed our results to be consistent with the action of injected muscimol on proximal lateral pulvinar neurons rather than on the distant LGN neurons.

Our injections were made in the visuotopic region of lateral pulvinar that contained central receptive fields (Fig. 1g, Supplementary Figs. 3 and 4). The part of dorsomedial LGN closest to the centre of these lateral pulvinar injections represents the lower visual field; more central LGN receptive fields are located posterolaterally further away from the centre of these injections (Supplementary Fig. 4). As LGN and V1 receptive fields are retinotopically co-located, if the suppression of V1 responses were mainly due to leakage of muscimol into LGN, then V1 receptive fields in the lower field must necessarily be affected in order for the more central receptive fields to be affected. In the three cases described above, the injection almost completely suppressed visual responses in central V1 receptive fields. However the more eccentric a V1 receptive field was in the lower field, the more responsive it was to visual stimulation (Supplementary Fig. 7). This spatial gradient of the effect of the injection on V1 is also consistent with proximal action of muscimol on lateral pulvinar rather than its leakage into LGN.

LGN activity during inactivation of lateral pulvinar

To further ensure LGN input to V1 was not accidentally disrupted by the lateral pulvinar injection, we performed two more direct controls. First, we injected into lateral pulvinar a fluorophore conjugated muscimol (FCM, Methods) instead of the muscimol-BDA mixture. FCM is a single molecule in which the muscimol terminus binds to the GABA receptor and the BODIPYR TMR-X terminus fluoresces near 572 nm, allowing us to determine the spatial extent of inactivation directly from the fluorescence (Fig. 2a, Methods).

Second, we monitored the integrity of LGN input to V1 by simultaneously measuring visual responses from LGN and V1 neurons both before and after the lateral pulvinar injection. To ensure that the measured LGN activity was largely responsible for the V1 activity assessed by the array, we selected LGN neurons with receptive fields completely overlapping those of the sampled V1 neurons[33]. One example is shown for measurements made before lateral pulvinar injection (Fig. 2b, top row). Simultaneously measured responses for an ipsilateral magnocellular LGN neuron (site “1” in layer Mi, Fig. 2a) and 7 superficial layer V1 neurons (Fig. 2b, top row) all of whose receptive fields were completely overlapping were both brisk, with peak-to-baseline ratios of 18 and 3.68 ± 0.02, respectively. Another example is shown for measurements made after lateral pulvinar injection (Fig. 2b, bottom row). The LGN response of this ipsilateral parvocellular neuron (site marked “2” in layer Pi, Fig. 2a) was still brisk, with peak-to-baseline ratio of 17 but the simultaneously measured V1 responses were suppressed, with a peak-to-baseline ratio of 0.46 ± 0.18 (Fig. 2b, bottom row).

Several LGN sites were sampled both before and after the lateral pulvinar injection. For each site, responses of a LGN neuron were measured simultaneously with several V1

neurons whose receptive fields overlapped that of the LGN neuron. The peak-to-baseline ratio did not change significantly for LGN neurons after lateral pulvinar injection (Wilcoxon rank-sum test, $P>0.39$; before lateral pulvinar injection: $n=8$, mean ± s.e.m = 15.31 ± 5.25; after lateral pulvinar injection: $n=14$, 15.08 ± 0.02; Fig. 2c). For V1 neurons, the ratio changed significantly after lateral pulvinar injection (Wilcoxon rank-sum test, $P< 10^{-6}$; before lateral pulvinar injection: $n = 52$, mean ± s.e.m = 5.32 ± 0.24; after lateral pulvinar injection: $n = 84$, 0.70 ± 0.04; Fig. 2c). These two controls showed that the integrity of LGN input to V1 was not compromised by the lateral pulvinar injection. The post-injection measurements included in the above analyses started 37 min after lateral pulvinar injection and finished 3 hours later. Throughout this period, LGN was robustly responsive to visual stimulation.

Sham and GABA injections

To verify that the mechanics of making the injection did not compromise V1 measurements (e.g., by displacing the electrode array during the insertion of the injectrode; see Methods), we performed 2 additional controls. First, while measuring the visual responses of V1 neurons with the array, we inserted the injectrode at the Horseley-Clarke co-ordinates for lateral pulvinar (Methods) and made a sham injection of the muscimol+BDA cocktail at a distance of 1.2 mm above the dorsal surface of lateral pulvinar (Fig. 3a; 1 animal). Peak-to-baseline ratios did not change significantly after the injection ($n = 44$, Wilcoxon rank-sum test, $P>0.5$; Fig. 3b). This confirmed that the injection process did not adversely affect V1 measurements.

Second, we injected into lateral pulvinar the fast and short acting native inhibitory transmitter GABA instead of the slow and long acting $GABA_A$ receptor agonist muscimol. Each injection of 0.4 μL of GABA in lateral pulvinar resulted in an immediate and drastic reduction in the visual responses of superficial layer V1 neurons (Fig. 3c). When injection was paused, stimulus-driven activity was immediately and fully restored in these neurons (Fig. 3c). We examined the responses of V1 neurons averaged within three distinct epochs: 1. pre-injection (~200 Sec – 1200 sec, Fig. 3c) 2. peri-injection (~1200 sec – 1600 sec, Fig. 3c) and 3. post-injection (~1600 sec – 2800 sec, Fig. 3c). Average response significantly changed (Wilcoxon rank-sum test, $P<0.007$, $n = 31$) from the pre-injection period (10.2 ± 1.7 spikes/sec) to the peri-injection period (5.4 ± 1.4 spikes/sec), a decrease of 47%. Average response also significantly changed (Wilcoxon rank-sum test, $P<10^{-4}$, $n = 31$) from the peri-injection period to the post-injection period (10.9 ± 1.7 spikes/sec), an increase of 101%. This quick and complete recovery once again confirmed that the injection process did not compromise V1 measurements. The almost instantaneous effect that these small volume (400 nL) GABA injections had on V1 responses also fairly effectively ruled out leakage into LGN as the source of suppression of V1 responses. Histology confirmed the injections were within lateral pulvinar and did not leak into LGN (Supplementary Fig. 8). Additionally, this experiment also showed that injecting $GABA_A$ receptor ligands with different molecular structures into lateral pulvinar obtain similar effects on V1 responses. Finally, the results of this experiment are consistent with a previous study that reported reduction in V1 responses after injection of GABA into the Lateral Posterior (pulvinar) complex of the cat[34].

Effect of focal excitation of lateral pulvinar

We also measured visual responses in supra-granular V1 layers while focally exciting lateral pulvinar neurons (2 animals). Drifting sinusoidal gratings were presented inside V1 receptive fields at the lower contrast of 14% (to reduce saturation effects) and at near-optimal orientations. To excite lateral pulvinar, we injected 0.4 μL of the $GABA_A$ receptor antagonist Bicuculline Methiodide (BMI). We compared V1 measurements from a 10 minute interval prior to the injection with measurements from a 13–15 minute interval after the injection (Fig. 4a). V1 receptive fields sampled by the array overlapped those of the injected lateral pulvinar neurons to varying extents. The baseline activity of all V1 neurons whose receptive fields were within 4°–6° of the injected lateral pulvinar receptive fields changed significantly after injection (53 neurons from 2 animals; Wilcoxon rank-sum, $P<0.008$), with an average increase of 72%.

For each V1 neuron, we normalized PSTHs over the entire 25 minute measurement period including the pre- and post-injection intervals (Fig. 4a). Normalized PSTHs were then averaged across neurons for the pre- and post-injection periods separately. In V1 neurons whose receptive fields were fully enveloped by the injected lateral pulvinar receptive fields and were fully stimulated by the visual stimulus (Fig. 4b), the ratio of peak-to-baseline response changed significantly (Wilcoxon rank-sum, $P<10^{-30}$; $n=14$), increasing by 232% from 2.8 ± 0.40 to 9.3 ± 0.02 (Fig. 4b). V1 neurons whose receptive fields overlapped those of the injected lateral pulvinar neurons by less than ~60% showed a suppression of response as a consequence of the injection (Fig. 4c). The peak-to-baseline ratio changed significantly (Wilcoxon rank-sum, $P<0.007$; $n=22$; Fig. 4c), decreasing by 83% to 0.47 ± 0.01. In V1 neurons whose receptive fields were fully enveloped by the injected lateral pulvinar fields but were only marginally stimulated by the visual stimulus that was centered on the lateral pulvinar receptive fields (Fig. 4d), the peak-to-baseline response changed significantly (Wilcoxon rank-sum, $P<0.01$; $n=17$), increasing by 483% from 1.2 ± 0.08 to 7.05 ± 0.60 (Fig. 4d). This latter group of V1 neurons behaved as if their receptive fields had either enlarged or shifted towards the center of the injected lateral pulvinar receptive fields or both (Fig. 4d). For fully stimulated V1 receptive fields (i.e., Figs. 4b and 4c), a regression analysis showed the effect of the receptive field overlap on the peak-to-baseline ratio to be significant ($R^2=0.64$; $F=66.5$; $P=0$; *variance*=0.13). In order to classify V1 receptive fields unambiguously into these three qualitative categories (Figs. 4b, c, d), only V1 neurons whose receptive fields were less than half the size of the injected lateral pulvinar receptive field were selected for these post-hoc analyses.

Histology showed the BMI injections were localized within lateral pulvinar and did not diffuse into LGN (Supplementary Fig. 9). All three types of significant changes observed in V1 responses (i.e., Figs. 4b, c, d) occurred within minutes (~2 min) of small volume (400 nL) BMI injections in lateral pulvinar. This quick onset was consistent with the observed changes in V1 being due to the action of injected material on proximal lateral pulvinar neurons rather than due to leakage into distant LGN neurons. To further verify that leakage of the excitatory agent into LGN was not involved in kindling V1 neurons, we performed a control in which we injected the LGN first and lateral pulvinar next with ibotenic acid, a glutamate agonist, and observed the effect on neurons in the supra-granular layers of V1

(Fig. 5a). Baseline activity was continuously measured with an electrode array in layers 2–3 of V1. We injected a large 1.8 μL volume of ibotenic acid into all layers of LGN covering the region of visual space spanned by the receptive fields of V1 neurons sampled by the array. LGN excitation by ibotenic acid first produced a burst of 8-fold increase in V1 activity (Figs. 5b; Wilcoxon rank-sum, P=0, n=39). The excitotoxic apoptosis of LGN neurons that followed caused a significant change in V1 baseline activity (Wilcoxon rank-sum, $P<10^{-30}$, n=39), with an average decrease of 85%. After allowing 30–60 minutes for the apoptotic lesion of LGN to complete, we injected 1.0μL of ibotenic acid into lateral pulvinar (Fig. 5a). Despite the significantly lower baseline activity, V1 neurons again showed a burst of 14-fold increase in activity following this lateral pulvinar injection (Figs. 5b; Wilcoxon rank-sum, P=0, n=39). Fluoro-Jade C® staining of degenerating neurons confirmed the location and extent of excitotoxic lesions in LGN and lateral pulvinar (Fig. 5a; Methods). The results of this control experiment fairly effectively ruled out LGN's involvement in the excitatory kindling of V1 neurons and are consistent with the report that electrical stimulation of pulvinar elicits positive BOLD response in V1 of the macaque[35].

Discussion

Our data show that removal of lateral pulvinar input can almost extinguish visual responses in the primary visual cortex and prevent the associated visual information from propagating beyond V1. The data also show that lateral pulvinar neurons can strongly boost V1 visual responses in the region of their receptive fields while suppressing responses to the surrounding region. These results suggest that the higher-order thalamic nucleus pulvinar plays a critical and integral part in the functioning of the visual cortex[36].

The spatial proximity of lateral pulvinar to LGN in the thalamus posed considerable technical challenges in our study. Taken together, the extensive histological analyses of the injections (Fig. 1g, Fig. 2a, Supplementary Figs. 3, 4, 8 and 9), the temporal dynamics of changes in V1 responses following the injection of muscimol in lateral pulvinar (Supplementary Figs. 5 and 6), the spatial gradient of changes in visual responses across the central 6° of V1 following the injection of muscimol in lateral pulvinar (Supplementary Fig. 7), the use of fluorescent muscimol to directly determine the spatial extent of inactivation from fluorescence (Supplementary Fig. 2a), direct simultaneous measurement of LGN and V1 responses following lateral pulvinar injections (Figs. 2b and 2c), the almost instantaneous effects that small volume (400 nL) injections of GABA and BMI had on V1 responses, and the excitatory kindling of V1 from lateral pulvinar after LGN lesion all implicate the manipulation of neural activity in lateral pulvinar as the cause of the observed effects in V1. However, as mentioned in Introduction, these experiments measured the *net* effect of manipulating lateral pulvinar activity on V1 and do not allow us to distinguish between the direct effect that lateral pulvinar exerts on V1 and the indirect effect exerted via pathways through higher visual cortex[4,36,37]. Nevertheless, our data reveal a surprisingly powerful scheme of control that the pulvinar can exercise over information processed and propagated within the visual cortex. Overall, our results illustrate a wide range of modulatory functions of a higher-order thalamic nucleus in cortical information processing[36]. Below, we briefly discuss possible relationships of these functions to circuits on the one hand and behavior on the other.

A role for lateral pulvinar in sustaining visual responses

How can lateral pulvinar effectively suppress geniculo-fugal visual input to V1? Quantitative accounting of our results requires more information, particularly about pulvinar afferents in V1 and the nature of lateral pulvinar's influence on V1 via the indirect pathway through extrastriate areas. However, some qualitative explanations can be suggested for how the direct pulvino-V1 circuit might be responsible for the observed effects. Several experimental and computational investigations indicate that a balanced combination of inhibitory and excitatory inputs underlies cortical neural responses[38–43]. Within this framework, our results could be accounted for if pulvinar provides potent excitatory synapses to V1. Many neurons in supra-granular layers that receive a disynaptic signal from the LGN will also receive a slightly delayed, quadrisynaptic geniculo-fugal signal via these lateral pulvinar synapses (Supplementary Fig. 10). Layer 5 cells in V1 that project to lateral pulvinar also receive input from supra-granular layers via their apical dendrites[44]. The resulting circuit may be lumped and depicted as consisting of a "loop" for computational purposes (Supplementary Fig. 10) though the system is clearly far more complex[36,45]. Under normal conditions, this pulvino-V1 "loop" might be necessary to drive and sustain the stimulus-evoked response. When lateral pulvinar is inactivated, the loss of the few but potent excitatory inputs from lateral pulvinar could result in a net inhibition that prevents visual responses from fully emerging. Stronger inhibition at the preferred orientation of the neuron as postulated in some V1 models[42,43] would yield greater suppression of the visual response for the preferred orientation after lateral pulvinar inactivation.

A second possibility is that a gating signal from lateral pulvinar acts multiplicatively on the geniculo-fugal feed-forward excitatory signal. Setting this lateral pulvinar gating signal low would suppress the geniculo-fugal excitatory input. These two possibilities are not mutually exclusive as lateral pulvinar could gate feedforward excitatory inputs in a circuit with balanced net excitation and inhibition to the same effect. Thus, including lateral pulvinar inputs in current models of V1 circuitry and function might account for some of our results.

Pulvinar and control of bottom-up salience for attention

Lesion or chemical inactivation of pulvinar often results in deficits of visual attention[12–20,23,24]. Electrophysiological and imaging assays of pulvinar neural activity have also shown links to visual attention[6,20,23–26]. Furthermore, pulvinar has reciprocal connections with both prefrontal and visual cortices[5]. These facts suggest a role for pulvinar in mediating visual attention which requires coordinated control of top-down and bottom-up signal flows[46]. Specifically, pulvinar sub-nuclei interconnected with early visual areas could control stimulus-driven or bottom-up salience of visual responses in conjunction with goal-driven or top-down signals received via the sub-nuclei interconnected with pre-frontal and parietal areas[15,47,48].

A network model of visual attention has postulated that pulvinar controls and routes information within the window of attention up the visual cortical hierarchy by gating feedforward synapses[48]. Our data show that lateral pulvinar can control and gate V1 neural activity in a manner consistent with its hypothesized role in controlling bottom-up salience for selective attention. When the spatiotemporal context of a visual stimulus autonomously

enhances its salience in conflict with behavioural or top-down goals, lateral pulvinar can suppress neural responses to this stimulus in early visual cortex (Fig 1), thus biasing the competition in favour of behaviourally-relevant stimuli[46]. When the window of attention is on a particular set of visual inputs, lateral pulvinar can boost neural responses to these inputs while simultaneously suppressing responses to surrounding inputs (Fig 4), thus gating and routing attended signals up the cortical hierarchy[48]. This analogy between our results and models of visual attention has an important caveat. The large changes in activity observed in our experiments as a consequence of direct pharmacological manipulation of lateral pulvinar need not necessarily be commensurate with the magnitude of neural effects measured in behavioural experiments in which changes in activity are governed not only by engaging or disengaging attention but also by other variables like attentional load, the spatiotemporal window of attention, and fixational eye movements.

Behavioral consequences of pulvinar inactivation

Our data show strong suppression of V1 visual responses following the reversible inactivation of a retinotopic region of lateral pulvinar. There are important caveats in inferring the behavioral consequences of this result. Reversible inactivation or lesion of pulvinar in awake behaving animals and humans may or may not reveal a scotoma depending on many factors including whether the affected region is restricted to parts of pulvinar that connect with early visual cortex or if it covers other sub-nuclei as well (e.g., in the macaque ventro-lateral and centro-lateral but not dorsomedial part of the lateral pulvinar connect to areas V1 and V2[5]), whether the subject is fixating or free-viewing, whether viewing is binocular or monocular (if pulvinar inactivation/lesion is unilateral), the retinotopic size of the affected area relative to the range of allowed fixational eye movements, and whether measurements are made after possible reorganization[16–18]. Another critical issue in the emergence of a scotoma is the size of the affected region and the nature of the background against which it is assessed[49]. Lesions to sub-nuclei connected to higher cortical areas (e.g., the dorsomedial part of lateral pulvinar[5]) are likely to have different types of behavioral consequences reflecting the functional properties of their projection zones[20,12–16]. Therefore, while it is hard to predict what the behavioral consequences of our results might be, our data clearly show that higher-order thalamic nuclei such as the pulvinar have a much more significant and key role to play in the cortical processing of sensory information than previously thought.

METHODS

Ten adult prosimian primates (*Otolemur garnettii*) of both sexes weighing 0.9–1.3 kgs were used in these experiments according to approved protocols from the IACUC at Vanderbilt University. Anesthesia was induced by an intraperitoneal injection of 30% Urethane solution (1.25 gms/kg) and maintained with 20% of induction dose every 2 hours. Neuromuscular blockade was achieved with Vencuronium bromide (0.5–1.0mg/kg/hr). Animals respired room air via a ventilator, supplemented with O_2 as necessary, to maintain expired CO_2 at 4%. Pupils were dilated with 2% cyclopentolate drops and contact lenses with sufficient power and 3-mm pupils were fitted to keep the monitor in clear focus on the retina.

Electrophysiology

V1 measurements were made using an electrode array. The dura was reflected and a Cyberkinetics 100 electrode array (Blackrock microsystems, Salt Lake City, UT) was pneumatically inserted over V1 and secured with 1% agarose in saline. Spikes were collected using a Bionics multichannel neural data acquisition system (Salt Lake City, UT) and sorted offline using Bayesian clustering methods (Plexon Inc). LGN and pulvinar measurements were made with single electrodes using a 16-channel Plexon Multichannel Acquisition Processor (Dallas, TX). Simultaneous measurements in V1 and LGN were made using differential mode recordings on both multichannel systems with common reference. We included in the analyses every neuron whose stimulus-driven PSTH (before lateral pulvinar injection) deviated outside the 95% confidence interval about the mean baseline response (for the analyses following the BMI injections, an additional selection criterion based on receptive field size was used as mentioned in that Results sub-section).

Receptive field mapping

In order to accurately map receptive fields, we used a modified version of Bishop's plotting table method (Bishop P.O, Henry, G.H, & Smith, C.J. *J. Physiol*., **216**, 39–68, 1971). Optic disks and retinal blood vessels were back reflected with a fiber-optic light source and plotted on a tangent screen 57 cm in front of the eyes. *Area centralis* (AC) was marked relative to the optical disk for each eye. Throughout the experiment, the positions of retinal landmarks were periodically checked for residual drifts of the paralyzed eyes. Stimuli such as moving lines, flashing lines, and flashing spots were created using a projector with analog controls and back projected onto the tangent screen. V1 receptive fields were then accurately hand mapped using these stimuli and plotted on the tangent screen along with retinal landmarks and the AC. Using a 45° mirror, the receptive fields, AC, and retinal landmarks were then precisely transferred to a CRT monitor on which experimental stimuli were presented.

Visual Stimuli

Visual stimuli were generated using a VSG 2/5 system (Cambridge Research, U.K.) and presented on a 22 inch Sony CRT display at 120 HZ refresh rate. Sinusoidal gratings at the behaviorally optimal spatial (0.5 cycles/degree) and temporal frequency (2 Hz) were presented at orientations varying from 0° to 170° in steps of 10°. Each orientation, randomly selected, was presented for 1 second followed by a 1 second inter-stimulus interval during which the monitor was at the mean luminance of 12 cd/m^2. Gratings covered V1 receptive fields of interest, were presented at 50% contrast in lateral pulvinar inactivation experiments, and at 14% contrast in experiments in which lateral pulvinar was excited. Simultaneous V1 and LGN measurements were made by finding an LGN neuron whose receptive field was completely inside V1 receptive fields of interest. A circular patch of light at high contrast (>90%) was flashed inside the LGN receptive field for 0.5–1 second followed by an equal duration inter-stimulus interval during which the monitor was at the mean luminance of 12 cd/m^2.

Injections

The central representation of LGN was first found using a single electrode, often by aiming for the posterior pole of the LGN at the Horsley-Clarke coordinates of AP +3 and ML +7. Central representation in lateral pulvinar was then found by moving 1.5 mm more medial (see Atlas of bush baby thalamus/pulvinar: http://www.psy.vanderbilt.edu/faculty/Casagrande/CasagrandeLab/BUSHBABYATLAS2.pdf). Receptive fields of lateral pulvinar neurons at this site were then accurately plotted. The electrode was replaced with a custom injectrode back-filled with the required cocktail. Previously mapped receptive fields were found again with the injectrode. The injectrode was then lowered by about 100 μm so that the tip of the pipette and not just the tip of the electrode reached the target. The injectrode was then pulled back by 100 μm and the cocktail was slowly infused. Pulling back the injectrode in this manner helps create a "pocket" within which the injected material stays confined, as indicated by dozens of cases of histology performed in our lab. *Muscimol injections* contained a 66.7mM solution of Muscimol (114MW; Sigma Aldrich) in a 1.6% solution of BDA (10000MW; Invitrogen). *GABA injections* contained a 25mM solution of GABA (103MW; Sigma Aldrich) in a 1.6% solution of BDA. *Bicuculline injections* contained a 5mM solution of BMI (509MW; Sigma Aldrich) in a 1.6% solution of BDA. *Fluorophore conjugated muscimol injections* contained 1 mg of muscimol, BODIPYR TMR-X conjugate (Invitrogen) dissolved in 1 ml of 0.9% saline. *Ibotenic acid injections* contained a 5mg/ml solution of ibotenic acid (158MW; Sigma Aldrich).

Histology

Sodium pentobarbital (Nembutal, 50–75 mg/kg) was used for euthanasia. Animals were perfused through the heart with a saline rinse containing 0.05% sodium nitrite, followed by a fixative (2% paraformaldehyde in 0.1M phosphate buffer or 3% Paraformaldehyde, 0.1% Gluteraldehyde and 0.2% saturated picric acid) and a 10% sucrose solution. The brain was blocked coronally with a blade mounted at a known coordinate in a stereotax. The occipital cortex was removed and flattened between slides in 0.1M phosphate buffer with 30% sucrose. Flattened pieces were frozen and tangentially sectioned. The surface vasculature was preserved in the first 100μm–150μm section. The remaining tissue was sectioned at 52μm. The thalamus was cut coronally. All sections were placed in 20% glycerol in 0.1M Tris buffered saline (TBS) and frozen at −70° C until staining. Cytochrome oxidase (CO) staining was used to confirm that the array was in the primary visual cortex (Supplementary Fig. 2). CO staining was performed by incubating sections in 0.2% DAB (D5636, Sigma), 0.3% Cytochrome C (250600, Calbiochem), 0.15% Catalase (C40, Sigma), 2% Sucrose, 0.03% $CoCl_2$ and 0.03% $NiNH_4SO_3$ in 0.05M Phosphate Buffer at 40° C for 1–4 hours until well differentiated. Tangential slices of the primary visual cortex stained for CO were successively examined to confirm that the electrode tips were within layers 2–3 (Supplementary Fig. 2). *AChE* The standard method of Karnovsky and Roots[50] was used. Sections were preincubated in 0.1 M Acetate buffer (pH 6.6), 0.1M Sodium Citrate, 20mM $CuSO_4$,10^{-3} M IsoOMPA, and 5mM $K_3Fe(CN)_6$ for 45 minutes. Sections were then incubated in a fresh solution as above with the addition of 0.1% ATHCH iodide overnight, rinsed in 0.1M Phosphate buffer, mounted on gelatinized slides, defatted, and cover-slipped with DPX. *BDA* To visualize BDA injected in the cocktails, sections were rinsed 3 times in

TBS, placed into 1:400 Alexafluor-488 conjugated Streptavidin (Invitrogen) in a buffer consisting of 0.1% Sodium azide, 0.2% Triton X 100 and 0.5% cold water fish gelatin for 2 hours, rinsed once in the same buffer, then twice in TBS. Sections were mounted and cover-slipped with Vectashield (Vector). *Fluoro-Jade® C* Sections were rinsed 3 times in TBS, mounted on subbed slides from distilled water (DH_2O), and placed on a 50° C slide warmer for a minimum of 30 minutes. They were then placed into 80% ethanol-1% Sodium hydroxide for 5 minutes, rinsed for 2 minutes in 70% ethanol, 2 minutes in DH_2O and then placed into 0.06% potassium permanganate in DH_2O for 10 minutes. They were rinsed in DH_2O for 2 minutes and transferred into a solution of 0.0001% Fluoro-Jade® C (Millipore) and 0.1% acetic acid in DH_2O. Slides were rinsed 3 times in DH_2O, dried on the slide warmer for a minimum of 5 minutes, cleared in Citrisolve (Fisher) for 5 minutes and cover-slipped.

Data Analysis

PSTHs were computed by aligning responses to stimulus onset, binning spikes in 50 ms intervals, and smoothing the binned averaged spike rate with a 150 ms wide sliding Gaussian window. The ratio of peak-to-baseline response was estimated as the ratio of the post-stimulus peak of the PSTH to the pre-stimulus PSTH values averaged over the 500 ms prior to stimulus onset. Suppression index at an orientation was estimated as the ratio of the peak-to-baseline value before injection to its value after injection.

Supplementary Material

Refer to Web version on PubMed Central for supplementary material.

Acknowledgments

We thank Julia Mavity-Hudson for the histology, Steven Walston, Yaoguang Jiang, Dmitry Yampolsky, Julia Mavity-Hudson, Jay Patel, and David Rinker for help with experiments, Dmitry Yampolsky for technical and computational assistance, and Mary Feurtado for veterinary assistance. We thank Drs. Ford Ebner, Jon Kaas, Romesh Khumbani, Jeff Schall, Pascal Wallisch, and King-Wai Yao for their suggestions and comments on the work. Supported by NIH grants R01-EY01778, P30-EY008126, T32-EY07135, and P30-HD15052.

References

1. Kandel, ER.; Schwartz, JH.; Jessell, TM. Principles of Neural Science. New York: McGraw-Hill; 2000.
2. Purves, D.; Augustine, GJ.; Fitzpatrick, D. Neuroscience. Sinauer Associates; 2004.
3. Van Essen DC, Anderson CH, Felleman DJ. Information processing in the primate visual system: An integrated systems perspective. Science. 1992; 255:419–423. [PubMed: 1734518]
4. Felleman DJ, Van Essen DC. Distributed hierarchical processing in primate cerebral cortex. Cereb Cortex. 1991; 1:1–47. [PubMed: 1822724]
5. Kaas JH, Lyon DC. Pulvinar contributions to the dorsal and ventral streams of visual processing in primates. Brain Res Rev. 2007; 55:285–296. [PubMed: 17433837]
6. Petersen DL, Robinson SE. Pulvinar and visual salience. Trends Neurosci. 1992; 15:127–132. [PubMed: 1374970]
7. Casanova, C. The visual functions of the pulvinar. In: Werner, JS.; Chalupa, LM., editors. The Visual Neurosciences. Cambridge, MA: MIT Press; 2004.

8. Benevento LA, Rezak M. The cortical projections of the inferior pulvinar and adjacent lateral pulvinar in the rhesus monkey (Macaca rnulatta): An autoradiographic study. Brain Res. 1976; 108:1–24. [PubMed: 819095]
9. Rezak M, Benevento LA. A comparison of the projections of the dorsal lateral geniculate nucleus, the inferior pulvinar and adjacent lateral pulvinar to striate cortex (area 17) in the macaque monkey. Brain Res. 1979; 167:19–41. [PubMed: 88245]
10. Ogren MP, Hendrickson AE. The distribution of pulvinar terminals in visual areas 17 and 18 of the monkey. Brain Res. 1977; 137:343–350. [PubMed: 412565]
11. Crick FC, Koch C. Constraints on cortical and thalamic projections: The no- strong-loops hypothesis. Nature. 1998; 391:245–250. [PubMed: 9440687]
12. Ward R, Danziger S, Owen V, Rafal R. Deficits in spatial coding feature binding following damage to the human pulvinar. Nature Neurosci. 2002; 5:99–100. [PubMed: 11780145]
13. Karnath H-O, Himmelbach M, Rorden C. The subcortical anatomy of human spatial neglect: putamen caudate nucleus and pulvinar. Brain. 2002; 125:350–360. [PubMed: 11844735]
14. Arend I, Machado L, McGrath M, Ro T, Ward R, Rafal R. The role of the human pulvinar in visual attention and action: evidences from temporal order judgment, saccade decision and anti-saccade tasks. Progress in Brain Research. 2008; 171:475–483. [PubMed: 18718343]
15. Snow JC, Allen HA, Rafal RD, Humphreys GW. Impaired attentional selection following lesions to human pulvinar: Evidence for homology between human and monkey. Proc Natl Acad Sci USA. 2009; 106:4054–4059. [PubMed: 19237580]
16. Chalupa LM. A review of cat and monkey studies implicating the pulvinar in visual function. Behav Biol. 1977; 20:149–67. [PubMed: 409388]
17. Ungerleider LG, Christensen CA. Pulvinar lesions in monkeys produce abnormal scanning of a complex visual array. Neuropsychologia. 1979; 17:493–501. [PubMed: 117393]
18. Bender DB, Butter CM. Comparison of the effects of superior colliculus and pulvinar lesions on visual search and tachistoscopic pattern discrimination in monkeys. Exp Brain Res. 1987; 69:140–154. [PubMed: 3436384]
19. Rafal RD, Posner MI. Deficits in human visual spatial attention following thalamic lesions. Proc Natl Acad Sci USA. 1987; 84:7349–7353. [PubMed: 3478697]
20. Wilke M, Turchi J, Smith K, Mishkin M, Leopold DA. Pulvinar inactivation disrupts selection of movement plans. J Neurosci. 2010; 30:8650–8659. [PubMed: 20573910]
21. Fischer J, Whitney D. Precise discrimination of object position in the human pulvinar. Hum Brain Mapp. 2009; 30:101–111. [PubMed: 17990302]
22. Smith AT, Cotton PL, Bruno A, Moutsiana C. Dissociating vision and visual attention in the human pulvinar. J Neurophys. 2009; 101:917–925.
23. Desimone R, Wessinger M, Thomas L, Schneider W. Attentional control of visual perception: Cortical and subcortical mechanisms. Cold Spring Harbor Symposium on Quantitative Biology. 1990; 55:963–971.
24. Petersen SE, Robinson DL, Morris JD. Contributions of the pulvinar to visual spatial attention. Neuropsychologia. 1987; 25:97–105. [PubMed: 3574654]
25. Bender DB, Youakim M. The effect of attentive fixation in macaque thalamus and cortex. J Neurophys. 2001; 85:219–234.
26. Kastner S, et al. Functional imaging of the human lateral geniculate nucleus and pulvinar. J Neurophysiol. 2004; 91:438–448. [PubMed: 13679404]
27. Wilke M, Mueller KM, Leopold DA. Neural activity in the visual thalamus reflects perceptual suppression. Proc Natl Acad Sci U S A. 2009; 106:9465–9470. [PubMed: 19458249]
28. Berman RA, Wurtz RH. Signals conveyed in the pulvinar pathway from superior colliculus to cortical area MT. J Neurosci. 2011; 31:373–384. [PubMed: 21228149]
29. Ivanov I, et al. Morphological abnormalities of the thalamus in youths with attention deficit hyperactivity disorder. Am J Psychiatry. 2010; 167:397–408. [PubMed: 20123910]
30. Mize RR, White DA. [^{3}H]Muscimol labels neurons in both the superficial and deep layers of cat superior colliculus. Neurosci Letters. 1989; 104:31–37.

31. Martin JH. Autoradiographic estimation of the extent of reversible inactivation produced by microinjection of lidocaine and muscimol in the rat. Neurosci Lett. 1991; 127:160–164. [PubMed: 1881625]
32. Hikosaka O, Wurtz RH. Modification of saccadic eye movements by GABA-related substances II. Effects of muscimol in monkey substantia nigra pars reticulata. JNeurophysiol. 1985; 53:292–308. [PubMed: 2983038]
33. Reid RC, Alonso JM. Specificity of monosynaptic connections from thalamus to visual cortex. Nature. 1995; 378:281–284. [PubMed: 7477347]
34. Molotchnikoff S, Shumikhina S. The lateral posterior-pulvinar complex modulation of stimulus-dependent oscillations in the cat visual cortex. Vision Res. 1996; 36:2037–2046. [PubMed: 8776470]
35. Logothetis NK, Augath M, Murayama Y, Rauch A, Sultan F, Goense J, Oeltermann A, Merkle H. The effects of electrical microstimulation on cortical signal propagation. Nature Neurosci. 2010; 13:1283–1291. [PubMed: 20818384]
36. Sherman SM, Guillery RW. Distinct functions for direct and transthalamic corticocortical connections. J Neurophysiol. 2011; 106:1068–1077. [PubMed: 21676936]
37. De Pasquale R, Sherman SM. Synaptic Properties of Corticocortical Connections between the Primary and Secondary Visual Cortical Areas in the Mouse. J Neurosci. 2011; 31:16494–16506. [PubMed: 22090476]
38. McCormick, DA.; Shu, YS.; Hasenstaub, A. Balanced recurrent excitation and inhibition in local cortical networks. In: Hensch, T., editor. Excitatory-Inhibitory Balance: Synapses, Circuits, Systems. Kluver Academic Press; New York: 2003.
39. Ferster D. Orientation selectivity of synaptic potentials in neurons of cat primary visual cortex. J Neurosci. 1986; 6:1284–1301. [PubMed: 3711980]
40. Softky WR, Koch C. The highly irregular firing of cortical cells is inconsistent with temporal integration of random EPSPs. J Neurosci. 1993; 13:334–350. [PubMed: 8423479]
41. Borg-Graham L, Monier C, Fregnac Y. Visual input evokes transient and strong shunting inhibition in visual cortical neurons. Nature. 1998; 389:369–373. [PubMed: 9620800]
42. Somers DC, Nelson SB, Sur M. An emergent model of orientation selectivity in cat visual cortical simple cells. J Neurosci. 1995; 15:5448–5465. [PubMed: 7643194]
43. Mariño J, Schummers J, Lyon DC, Schwabe L, Beck O, Wiesing P, Obermayer K, Sur M. Invariant computations in local cortical networks with balanced excitation inhibition. Nat Neurosci. 2005; 8:194–201. [PubMed: 15665876]
44. Callaway EM. Local circuits in primary visual cortex of the macaque monkey. Ann Rev Neurosci. 1998; 21:47–74. [PubMed: 9530491]
45. Rockland KS. Convergence and branching patterns of round, type 2 corticopulvinar axons. J Comp Neurol. 1998; 390:515–536. [PubMed: 9450533]
46. Desimone R, Duncan J. Neural mechanisms of selective visual attention. Ann Rev Neurosci. 1995; 18:193–222. [PubMed: 7605061]
47. Van Essen, DC. Cortico-cortical and thalamo-cortical information flow in the primate visual system. Cortical Function: A View from the Thalamus. In: Casagrande, VA.; Guillery, R.; Sherman, M., editors. Progress in Brain Research. Vol. 149. Elsevier; 2005. p. 173-185.
48. Olshausen BA, Anderson CH, Van Essen DC. A neurobiological model of visual attention and invariant pattern recognition based on dynamic routing of information. J Neurosci. 1993; 13:4700–4719. [PubMed: 8229193]
49. Ramachandran VS, Gregory R. Perceptual filling in of artificially induced scotomas in human vision. Nature. 1991; 350:699–702. [PubMed: 2023631]
50. Karnovsky MJ, Roots L. A ‘direct coloring’ thiocholine method for cholinesterases. J Histochem Cytochem. 1964; 12:219–220. [PubMed: 14187330]

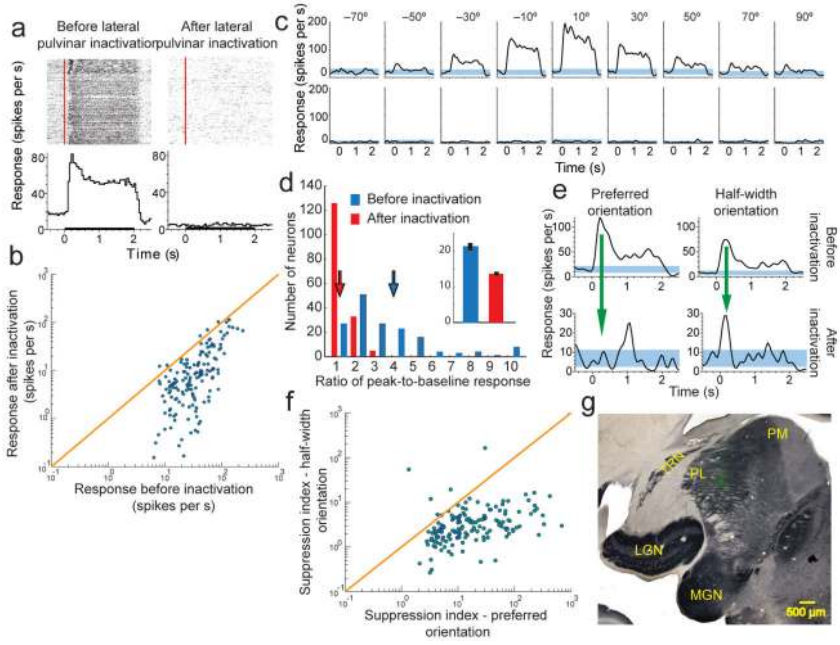

Figure 1. Reversibly inactivating lateral pulvinar almost abolishes visual responses in supragranular layers of V1

(a) Raster plots representing each spike as a dot and Peri-Stimulus Time Histograms (PSTHs) are shown for a sample neuron in layers 2–3 of V1 before (left column) and after (right column) lateral pulvinar inactivation. Red line on the raster plot shows visual input onset time and black line on the abscissa of the PSTH shows the visual input presentation time. Responses shown are for a drifting sinusoidal grating presented within the neuron's receptive field at 18 different orientations. (b) Comparison of the average input-driven response before and after lateral pulvinar inactivation for all 164 V1 neurons. (c) PSTHs are shown separately for 9 orientations at which this neuron was most responsive before lateral pulvinar inactivation. Blue bands represent 95% confidence interval around the mean baseline response measured before visual stimulation. (d) The phasic response, quantified as the ratio of peak-to-baseline activity, is shown for 164 V1 neurons before (blue) and after (red) lateral pulvinar inactivation. Inset shows baseline responses. (e) PSTHs are shown for a layer 3 V1 neuron before (top row) and after (bottom row) lateral pulvinar inactivation for the preferred orientation (left column) and half-width orientation (right column). Responses are shown at different scales for the top and bottom rows. (f) Comparison of suppression indices at preferred and half-width orientations for all 164 V1 neurons. (g) A composite figure showing the injection in lateral pulvinar. Coronal section of the left thalamus was stained for cytochrome oxidase (CO). A fluorescent image (green) was obtained with Alexafluor-488 conjugated streptavidin as probe for the BDA mixed with the muscimol injected in lateral pulvinar. The fluorescence image was used to create a vector mask for the CO image, thereby rendering transparent in the CO image all pixels with intensity above background in the fluorescent image. Fluorescence seen in the composite image is through these transparent pixels in CO. Fluorescence is localized well within lateral pulvinar and is more than 1 mm away from the TRN and LGN. LGN, lateral geniculate nucleus; MGN,

medial geniculate nucleus; PL, lateral pulvinar; PM, medial pulvinar; TRN, thalamic reticular nucleus.

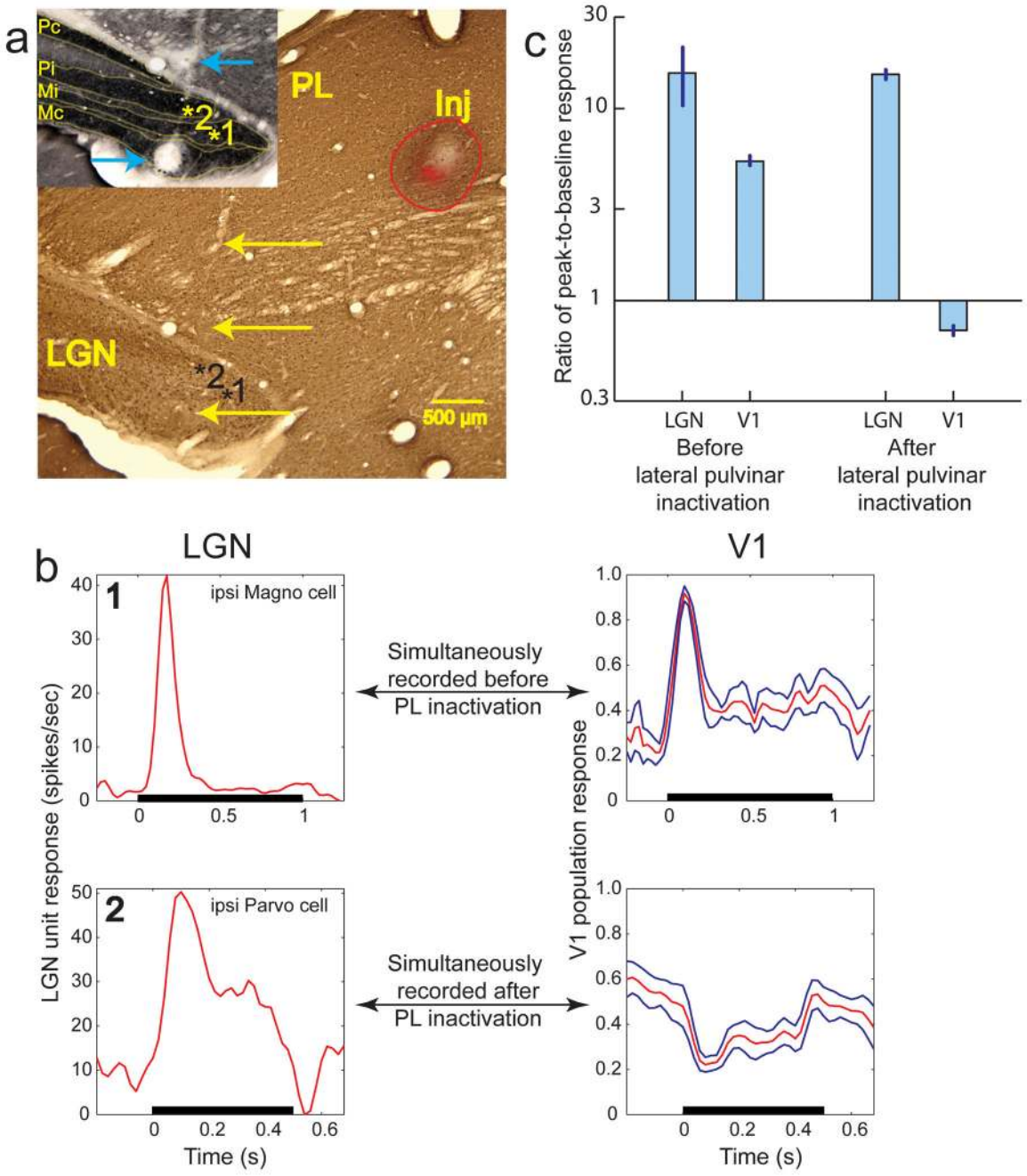

Figure 2. Absence of V1 output in the presence of LGN input

(a) Composite figure of the injection, created using the method mentioned above (Fig. 1g). Coronal section of left thalamus was stained for Calbindin. The injection in lateral pulvinar is labeled “Inj”. Red fluorescence is from fluorophore conjugated muscimol that was injected to inactivate this region of lateral pulvinar. The red outline shows the overall extent of the injection reconstructed from several successive sections through the thalamus. Region of inactivation is identical to the red fluorescent region, which is about 2 millimeters away from the LGN. The track from the electrode approaching LGN measurements sites is visible on the left. Yellow arrows mark 3 electrical lesions made along the electrode track for

locating measurement sites in LGN. Inset shows the CO stained adjacent section with LGN layers marked and labeled. Blue arrows mark the 2 most ventral lesions. Numbers on the marked sites correspond to the numbers on the PSTHs shown in (b). (b) PSTHs measured at 2 LGN sites are shown along with simultaneously measured V1 responses before lateral pulvinar inactivation (top row) and after (bottom row). PSTH of a LGN neuron from the ipsi magnocellular layer in site 1 shows a brisk-onset transient response to a 1 second long visual stimulation of its receptive field. The mean normalized PSTH of 7 supra-granular V1 neurons, whose receptive fields completely overlapped that of the simultaneously measured LGN neuron (on the left), is shown in red. Blue lines show 1 s.e.m. Measurements at site 2 in the ipsi parvocellular layer were made after the lateral pulvinar injection. PSTH measured at this LGN site is shown along with the mean normalized PSTH of the simultaneously measured V1 responses. (c) Average ratio of peak-to-baseline response is shown for 8 LGN and 52 V1 neurons before lateral pulvinar inactivation; 14 LGN and 84 V1 neurons after lateral pulvinar inactivation. Error bars show 1 s.e.m.

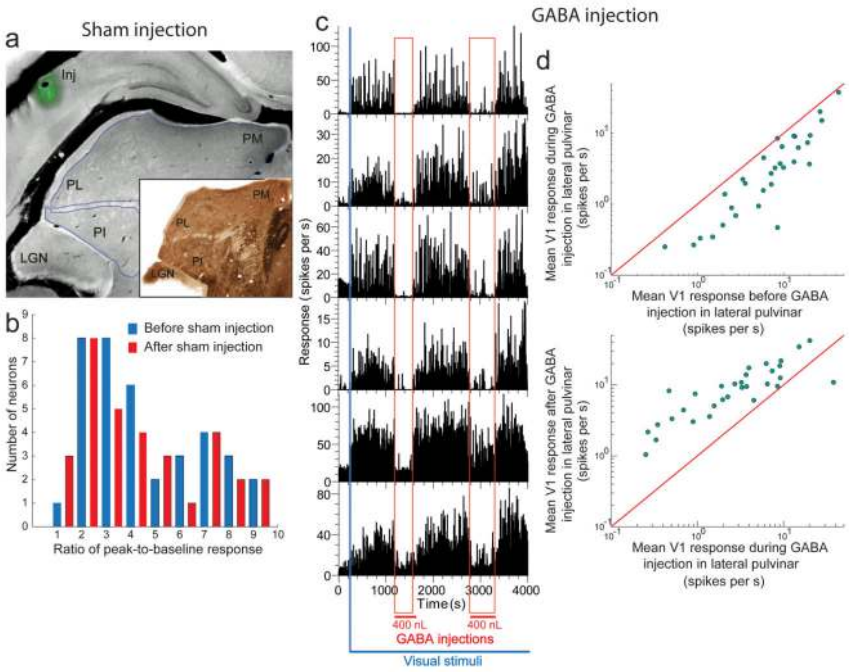

Figure 3. The process of lateral pulvinar injection does not compromise the integrity of V1 measurements

(a) Coronal section showing sham injection (Inj) above lateral pulvinar. (Inset) Adjacent section stained for AChE. (b) Ratio of peak-to-baseline response for 44 V1 neurons from layers 2–3 before (blue) and after (red) sham injection. (c) Effect of injecting in lateral pulvinar short-acting GABA on visually driven responses for layer 2–3 V1 neurons. The blue bar represents the beginning of presentation of the visual stimuli sequence consisting of a 1-second presentation of a drifting sinusoidal grating and a 1 second inter-stimulus interval. During this continuous visual stimulation of V1 neurons, two 400 nL injections of GABA were made in lateral pulvinar, about 1500 seconds apart. The time period of each injection is shown marked by the vertical red band. (d) Comparisons of mean V1 responses during the pre-injection and peri-injection periods (top) and the mean V1 responses during the peri-injection and post-injection periods (bottom). LGN, lateral geniculate nucleus; PL, lateral pulvinar; PM, medial pulvinar; PI, inferior pulvinar.

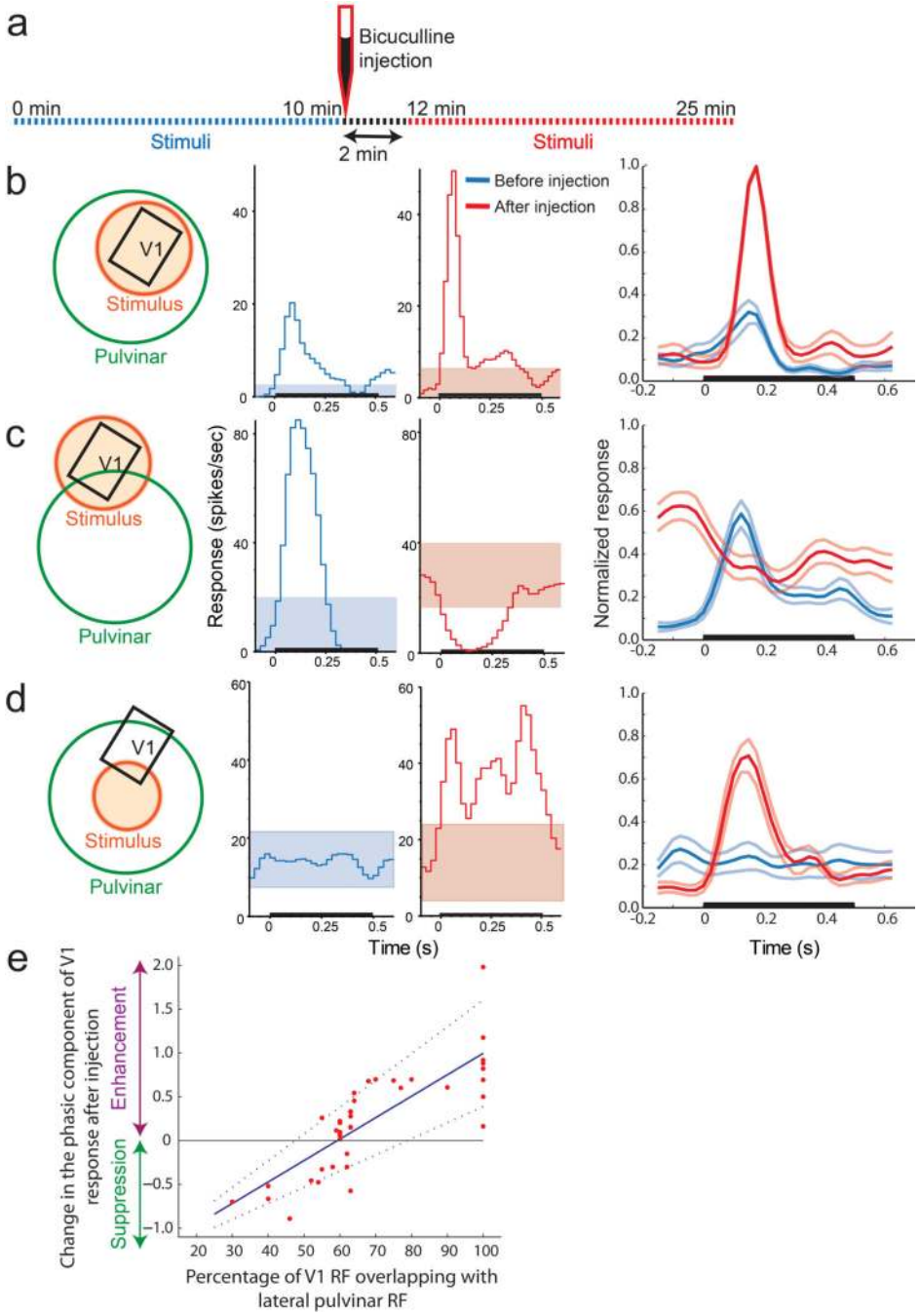

Figure 4. Exciting lateral pulvinar neurons responsive to a region boosts responses of V1 neurons to this region and suppresses responses to surrounding region

(a) Timing of response measurements and the injection of BMI. (b) In one subset of V1 neurons studied, V1 receptive fields (black) were enveloped by the injected lateral pulvinar receptive fields (green) and visual stimulation (orange) was centered on the V1 receptive fields. Visual responses of a V1 neuron with receptive field inside the excited lateral pulvinar receptive field are shown before (blue) and after (red) lateral pulvinar excitation. Colored bands represent 95% confidence interval about the baseline response. Last column shows the normalized responses of 14 V1 neurons in this subset, averaged over the pre-

injection (thick blue line) and post-injection (thick red line) periods. Lighter lines represent 1 s.e.m. (c) In the second subset of V1 neurons studied, visual stimulation (orange) was centered about their receptive fields (black) that overlapped with the injected lateral pulvinar receptive fields by less than 60%. Brisk visual responses obtained before lateral pulvinar injection (blue) were suppressed after the injection (red). Last column shows the average PSTHs for the pre-injection (blue) and post-injection (red) periods. The average PSTH before lateral pulvinar injection in this case (last column, thick blue line) appears slightly larger than that seen in (b) due to normalization with respect to smaller post-injection responses. (d) In the third subset of V1 neurons, visual stimulation (orange) was centered about the lateral pulvinar receptive field and was marginal for the V1 receptive fields. V1 receptive fields were enveloped by the injected lateral pulvinar receptive fields. V1 neurons that hardly responded to the marginal stimulation of their receptive fields before lateral pulvinar injection (blue) showed a vigorous response after (red) the injection. (e) Change in the ratio of peak-to-baseline response is shown plotted on a logarithmic scale against the percentage of V1 receptive field overlapping with excited lateral pulvinar receptive field. Regression result is shown as the continuous blue line and the dotted lines represent 95% confidence interval for the estimate of the regression slope.

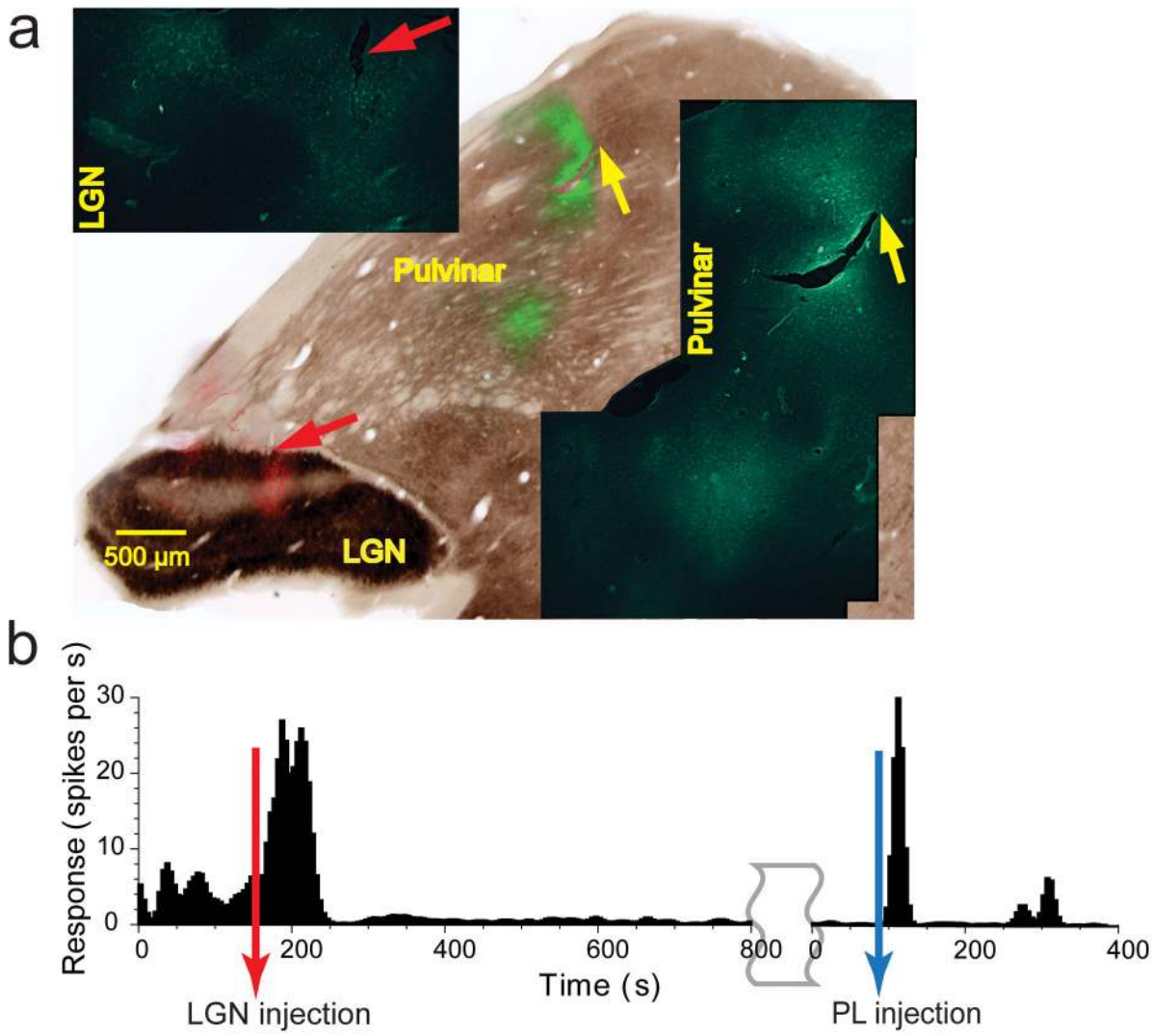

Figure 5. Kindling of V1activity by lateral pulvinar excitation after LGN lesion

(a) Composite image showing the injections, created using the method mentioned above (Fig. 1g). Coronal section stained for AChE showing ibotenic acid injections in false colors, green in lateral pulvinar and red in LGN. Insets show regions of injections stained with Fluoro-Jade CR in higher magnification. Individual degenerating cells are seen labeled. (b) Changes in the baseline response of a supra-granular V1 neuron due to the injection of ibotenic acid in LGN and lateral pulvinar. The lateral pulvinar injection was made 30 mins after the end of the timeline shown for the LGN injection.